Therapeutics, Targets, and Chemical Biology

Cancer Research

Blockade of Tumor Necrosis Factor α Signaling in Tumor-Associated Macrophages as a Radiosensitizing Strategy

Yuru Meng[1], Michael A. Beckett[1], Hua Liang[1], Helena J. Mauceri[1], Nico van Rooijen[3], Kenneth S. Cohen[2], and Ralph R. Weichselbaum[1]

Abstract

Most cancer patients receive radiotherapy during the course of their disease. Improvements in the therapeutic index have been based mainly on physical improvements in delivery, as radiosensitizer development to target tumor cells has yet to yield effective agents. Recent investigations have focused on the tumor stroma as a target for radiosensitization. Here, we report that depletion of tumor-associated macrophages (TAMφ) by systemic or local injection of the macrophage-depleting liposomal clodronate before radiotherapy can increase the antitumor effects of ionizing radiation (IR), either as a large single dose (20 Gy) or as a fractionated dose (2 Gy × 10). Coimplantation of tumor cells with bone marrow–derived macrophages (BMDMφ) increased tumor radioresistance. Studies using mice with germline deletions in tumor necrosis factor receptors 1 and 2 (TNFR1,2$^{-/-}$) or TNFα (TNF$^{-/-}$), or treatment of wild-type mice with a soluble TNF receptor fusion protein (Enbrel), revealed that radioresistance mediated by BMDMφ required intact TNFα signaling. Radiation exposure upregulated vascular endothelial growth factor (VEGF) in macrophages and VEGF-neutralizing antibodies enhanced the antitumor response to IR. Thus, the radioprotective effect of TNFα was mediated by TAM-produced VEGF. Our findings offer a mechanistic basis to target macrophage populations generally or TNFα-induced macrophage VEGF specifically as tractable strategies to improve the efficacy of radiotherapy.
Cancer Res; 70(4); 1534–43. ©2010 AACR.

Introduction

Radiation therapy is a common cancer treatment usually delivered in a fractionated schedule (daily 1.8–3 Gy) for 6 to 8 weeks. In some selected lung cancers, or limited forms of metastasis, very large doses (one to five treatments of 10–20 Gy) may be used (1). Despite research into the radiobiology and physics of radiotherapy, many patients fail within the irradiated target volume. Currently, the most effective radiosensitizers represent the commonly used chemotherapeutic agents (2). These drugs are not designed as selective radiosensitizers, and clinical improvement reflected by increased local control is achieved at the expense of significant normal tissue toxicity. More selective radiosensitizing agents and new treatment strategies are required to improve the therapeutic index in radiotherapy.

Research on the mechanisms of tumor radioresistance and the development of radiosensitizers focuses on tumor cells or exploiting differences in the oxygenation status of tumors and normal tissue (3). Recently, the tumor-associated stroma has gained attention as an important component of the response to radiotherapy (4, 5) and investigations have centered on the role of the tumor-associated vasculature (6, 7). Several clinical trials are under way to investigate the role of angiogenesis inhibitors in combination with radiotherapy (8–11). The results are preliminary and, although promising, show mixed results in terms of improving radiotherapy outcomes and unexpected toxicities have been reported (11–13). Conversely, little is known about other components of the tumor-associated stroma and the effect of these cells on the response of tumors to radiotherapy.

Macrophages are multifunctional cells of the myeloid lineage, phenotyped as CD14^{+}. Macrophages engulf microbes and cell debris, are antigen-presenting cells, and secrete cytokines and chemokines. Macrophage function is described within the context of normal physiologic or pathologic microenvironments. Macrophages are designated as M1 classically activated macrophages or M2 alternatively activated macrophages. Proinflammatory M1 macrophages are activated by lipopolysaccharide and IFNγ, secrete tumor necrosis factor (TNF) α and interleukin (IL)-12, and support T-cell function. M2 macrophages are considered to be anti-inflammatory and

Authors' Affiliations: [1]Department of Radiation and Cellular Oncology and [2]Department of Medicine, Section of Hematology/Oncology, The University of Chicago, Chicago, Illinois and [3]Department of Molecular Cell Biology, VU University Medical Center, Vrije Universiteit, Amsterdam, the Netherlands

Note: Supplementary data for this article are available at Cancer Research Online (http://cancerres.aacrjournals.org/).

Y. Meng and M.A. Beckett contributed equally to this work.

Corresponding Author: Ralph R. Weichselbaum, Department of Radiation and Cellular Oncology, Duchossois Center for Advanced Medicine, 5758 South Maryland Avenue, MC 9006, Chicago, IL 60637. Phone: 773-702-0817; Fax: 773-834-7233; E-mail: rrw@radonc.uchicago.edu.

doi: 10.1158/0008-5472.CAN-09-2995

immunosuppressive, expressing F4/80, CD11b, and CD206; secrete IL-10, IL-4, and transforming growth factor-β; and downregulate T-cell function (14, 15). Tumor-associated macrophages (TAMφ) are usually characterized as M2. However, functional overlap exists between characteristics of M1 and M2 macrophages. Additional/expanded definitions of TAMφ populations have been investigated as determinants of tumor progression and metastasis. These populations include $CD11b^+/Gr1^+$ myeloid suppressor cells as well as $Tie2^+$-expressing macrophages (15, 16). Emerging data suggest key roles for these various monocyte/macrophage cells in generating proangiogenic signals during tumor growth.

Radiation was originally reported to prime the antitumor effects of macrophages through production of TNFα and nitric oxide (NO; refs. 17–20). However, Milas and colleagues investigated the association between TAMφ and the response of tumors to radiotherapy and noted a trend toward decreasing radiocurability with increasing TAMφ content. These investigators recognized the contradiction between potential beneficial (phagocytic function) and deleterious functions (proangiogenic phenotypes) of TAMφ (21–23). Recently, Tsai and colleagues (24) reported that irradiated macrophages contributed to tumor growth through increased secretion of cyclooxygenase-2, inducible NO synthase (iNOS), and Arg-1, although no direct mechanisms for promotion of tumor growth were described. Ahn and Brown (25) reported that cells of the myeloid/macrophage lineage contributed to tumor regrowth following radiation by increasing tumor vasculogenesis when tumor angiogenesis was suppressed by prior irradiation of the tumor bed. Collectively, these studies raise the possibility that macrophage populations contribute to tumor radioprotection. Moreover, radiation of the tumor microenvironment might upregulate macrophage-derived cytokines that promote tumor growth, survival, angiogenesis, and vasculogenesis.

TNFα, which has antitumor effects at high concentrations, also promotes tumor angiogenesis, tumor cell survival, and metastases at lower levels (26). A recent report suggested that TNFα mediates the differentiation of monocytes into angiogenic cells that support tumor angiogenesis (27–29). Radiotherapy, although directly inducing tumor cell death, may upregulate proangiogenic and prosurvival factors within the tumor microenvironment. We and others have found that radiation upregulates TNFα production by tumor cells and cells of the myeloid lineage (30, 31). Here, we report that depletion of macrophages by liposomal clodronate before irradiation increases the antitumor effects of ionizing radiation (IR), whereas coimplantation of tumor cells with bone marrow–derived macrophages (BMDMφ) results in increased tumor radioresistance. The radioprotective effect of BMDMφ requires functional TNFα/TNFR signaling and induction of macrophage-secreted vascular endothelial growth factor (VEGF). We report that blockade of macrophage VEGF induction by Enbrel (soluble TNF receptor dimeric fusion protein), used in several murine studies, increased tumor radiosensitivity (32, 33). We also report that blocking VEGF with neutralizing antibodies improves the antitumor effects of IR. These data provide a rationale for targeting macrophage populations generally and TNFα-induced VEGF signaling specifically when designing radiotherapeutic strategies.

Materials and Methods

Mice and tumor cell lines. C57BL/6 mice wild-type (WT), C57BL/6-129S-$Tnfrsf1a^{tm1Imx}Tnfrsf1b^{tm1Imx}$/J ($TNFR1,2^{-/-}$), B6:-129S-$Tnf^{tm1Gkl/J}$ ($TNF^{-/-}$), and C57BL/6-Tg (UBC-GFP) 30SchaJ ($GFP^{+/+}$) breeding pairs were purchased from The Jackson Laboratory. $TNF^{-/-}$ mice maintained in the 129/SvEv and C57BL/6 backgrounds after six-generation backcross have been previously used to study the effects of TNFα on tumor promotion and antigen presentation (29, 34). B16F1 melanoma cells were cultured as described (35) B16.SIY melanoma cells expressing model antigen SIY, which can be recognized by $CD8^+$ T cells in the context of K^b, were cultured as described. The care and treatment of experimental animals was in accordance with institutional guidelines.

Generation of BMDMφ. Femoral BM cells were obtained from mice and cultured in complete RPMI 1640 supplemented with 10% FCS and 30% pretested conditioned medium from the L929 cell line as a source of macrophage colony-stimulating factor (M-CSF) for the first 5 d followed by complete RPMI 1640 supplemented with 10% FCS and 10 ng/mL recombinant M-CSF (R&D Systems) for additional 5 d. These BMDMφ were >95% $CD14^+$ and >90% $CD11b^+F4/80^+$, analyzed by fluorescence-activated cell sorting (FACS).

Tumor induction and irradiation. Tumor cells (5×10^5 B16F1 or B16.SIY) were inoculated s.c. into the right hind limb. Tumors were measured with calipers and volume was calculated as length × width × depth/2. At days 10 to 12, local radiotherapy (single dose, 20 Gy; fractional doses, 2 Gy × 10) was delivered. In some experiments, B16F1/B16.SIY cells were coinjected with BMDMφ at a 4:1 ratio. Elsewhere, macrophages were depleted by i.p. or intratumoral administration of liposomal clodronate every 5 to 7 d (36). Cl_2MDP (or clodronate) was a gift of Roche Diagnostics GmbH (37). Other reagents include phosphatidylcholine (Lipoid GmbH) and cholesterol (Sigma). Macrophage depletion was confirmed by FACS and immunohistochemistry of spleen and tumor cryosections with >90% reduction compared with the control. Blockade of VEGF using neutralizing IgG against mouse VEGF-164 (R&D Systems) has been previously described (38). Briefly, goat IgG against mouse VEGF-164 was suspended in PBS and administered via i.p. injection (10 μg/mouse, 3 h before IR and 3 and 8 d after IR). Control mice received goat IgG (Sigma).

Colony-forming assay. Two hundred control or irradiated B16F1 or B16.SIY cells were seeded in 5-cm culture dishes in RPMI 1640 containing 10% FCS with or without 30% spent supernatant collected from either WT, $TNF^{-/-}$, or $TNFR1,2^{-/-}$ BMDMφ (5×10^6 cells). After 7 d, cells were washed and stained with crystal violet. Colonies with >50 cells were counted.

Protein array and Luminex. Spent culture supernatants were collected and incubated with membranes coated with 62 anti-mouse cytokine antibodies (RayBiotech, Inc.)

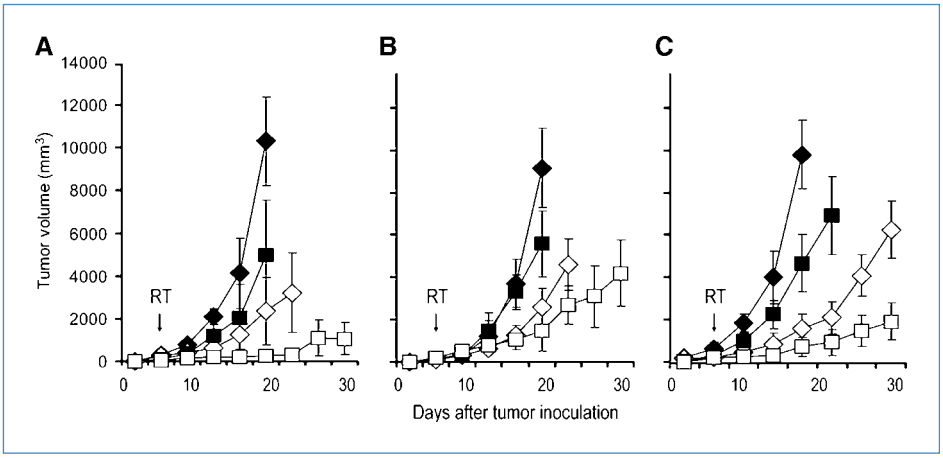

Figure 1. Depletion of macrophages enhances radiation. A, systemic macrophage depletion with liposomal clodronate (200 μL i.p.) before inoculation of B16.SIY cells significantly (P = 0.002) enhanced IR (20 Gy) compared with IR alone in WT (n = 11–16/group). B, systemic depletion of macrophages after tumors were established enhanced IR (P = 0.071) compared with IR alone (n = 11–16/group). C, intratumoral macrophage depletion significantly (P = 0.037) delayed tumor regrowth compared with IR alone (n = 10–12/group). ♦, liposomal PBS; ◇, 20 Gy + liposomal PBS; ■, liposomal clodronate; □, 20 Gy + liposomal clodronate.

according to the manufacturer's instruction. An antibody labeled with biotin coated on the upper left and lower right corners of the membrane served as positive control. The film was scanned and spots were quantified by densitometry analysis using UN-SCAN-IT gel automated digitizing system software (Silk Scientific). Thirty-two cytokines were quantified using Mouse Cytokine/Chemokine Premixed 32 Plex (Millipore). Median fluorescence intensity from each well was acquired, and the relative concentration of each cytokine/chemokine was calculated.

FACS and cell sorting. Tumors were excised, sectioned, and digested in DMEM supplemented with 2% FCS and 1.5 mg/mL collagenase D (Sigma) for 30 min in a 37°C shaking incubator to collect single-cell suspension. Cells were stained with anti-CD11b, anti-CD206, anti-F4/80, anti-TNFR1, and anti-TNFR2 (BioLegend); washed; and analyzed on a LSR flow cytometer. Frequency of $CD11b^+$ and $F4/80^+$ TAMφ was analyzed and sorted on a MoFlow to collect TAMφ. Purity reached >95% $CD11b^+$ $F4/80^+$ cells.

Western blot. Cells were lysed with cell lysis buffer containing 20 mmol/L Tris-HCl (pH 7.5), 150 mmol/L NaCl, 1 mmol/L Na_2EDTA, 1 mmol/L EGTA, 1% Triton, 2.5 mmol/L sodium pyrophosphate, 1 mmol/L glycerophosphate, 1 mmol/L Na_3VO_4, 1 μg/mL leupeptin, and protease inhibitor mixture (Roche Applied Science). Protein concentrations were determined using the Bio-Rad protein assay kit, and 10 μg from each sample were analyzed on 10% SDS-PAGE gels. Protein bands were transferred onto polyvinylidene difluoride membranes and probed with rabbit anti-mouse VEGF (Santa Cruz Biotechnology) for 2 h and then horseradish peroxidase–conjugated anti-rabbit for 1 h. Membranes were washed and immunodetected using ECL kit (Amersham Biosciences). Anti–β-actin-stained membranes were used as loading control.

Histopathology and immunohistochemistry. Tissues were fixed in 10% neutral formalin or 4% paraformaldehyde. Sections were blocked with 5% goat serum and incubated with VEGFR2 antibody (1:200 dilution; Cell Signaling Technology) for 1 h. After washing with TBS, biotinylated anti-rabbit secondary antibody followed by avidin-biotin complex–alkaline phosphatase (ABC-AP; Vector Laboratories) was applied for 30 min each. Vector blue substrate was used for color development. For the following NG2 chondroitin sulfate proteoglycan staining, the slides were washed and blocked with avidin-biotin blocking kit and then 10% goat serum for 10 min. Slides were incubated in 1:100 dilution of NG2 antibody (Millipore) overnight at 4°C. After applying biotinylated secondary antibody and ABC-AP solution, tissues were covered with Vulcan fast red substrate (Biocare Medical) for 15 min. Slides were washed and counterstained with methyl green. Sections were dehydrated in 100% ethanol, cleared by Histoclear (Wards Natural Science), and then mounted with VectaMount (Vector Laboratories). Images were photographed at ×200 magnification using a Zeiss camera operated by Openlab software.

Statistical analysis. A random-effects model for longitudinal data was used to obtain an overall estimate of the intercept and slope of linear growth for each group. One-way ANOVA with Dunnett's post test was performed using GraphPad InStat version 3.05 ($P < 0.05$).

Results

Depletion of macrophages increases the antitumor effects of IR. Macrophages were depleted by i.p. injection of liposomal clodronate (37) 1 day before injection of 2×10^6 B16.SIY cells and every 5 days thereafter in WT mice. Ninety percent of the macrophages were specifically depleted in the spleen and tumor microenvironment as analyzed by FACS (Supplementary Fig. S1; refs. 36, 39, 40). Twenty Gray was administered when tumors reached 150 to 200 mm^3. The combination of liposomal clodronate and 20 Gy significantly

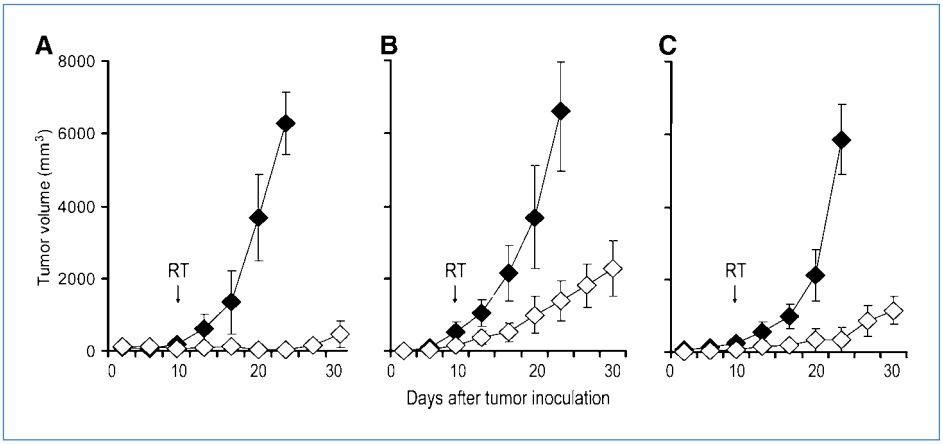

Figure 2. TNFα signaling in BMDMϕ mediates tumor radioresistance. A, baseline radiation response to 20 Gy of B16.SIY tumors growing in WT (n = 12/group). ⧫, B16; ◇, IR in B16. B, coinjection of WT BMDMϕ with B16.SIY tumor cells significantly accelerates tumor regrowth following 20 Gy compared with baseline (A; P = 0.03, n = 12/group). ⧫, WT macrophage + B16; ◇, IR in WT macrophage + B16. C, coinjection of $TNF^{-/-}$ BMDMϕ with B16.SIYcells significantly decreased tumor regrowth following 20 Gy compared with WT (B; P = 0.03, n = 12/group). ⧫, $TNF^{-/-}$ macrophage + B16; ◇, IR in $TNF^{-/-}$ macrophage + B16.

delayed tumor regrowth compared with 20 Gy alone (335 ± 207 mm^3 versus 3,215 ± 1,849 mm^3, day 22; P = 0.002) or liposomal clodronate alone (273 ± 198 mm^3 versus 4,987 ± 2,556 mm^3, day 18; P = 0.041; Fig. 1A). Liposomal clodronate also enhanced the antitumor effects of IR after tumors were established compared with 20 Gy alone (2,678 ± 1,243 mm^3 versus 4,599 ± 889 mm^3, day 22; P = 0.071; Fig. 1B). We also injected liposomal clodronate intratumorally and observed that tumor regrowth was significantly delayed compared with IR alone (1,669 ± 749 mm^3 versus 5,317 ± 1,322 mm^3, day 26; P = 0.037; Fig. 1C).

TNFα signaling in BMDMφ mediates tumor radioresistance. TNFα is reported to both enhance tumor growth and mediate antitumor effects. To study the role of TNFα produced by macrophages, we cultured BMDMφ from WT and $TNF^{-/-}$ mice and coinjected these BMDMφ with 5×10^5 B16.SIY cells into WT mice. $TNF^{-/-}$ and WT BMDMφ exhibit similar levels of cell surface markers with >95% CD14 and 90% CD11b detected by FACS. They also expressed similar levels of iNOS but $TNF^{-/-}$ BMDMφ expressed significantly lower levels of Arg-1 (data not shown). The percentages of $F4/80^+$ TAMφ were similar between the WT and $TNF^{-/-}$ groups, although $TNF^{-/-}$ cells had diminished levels of surface CD206 staining (Supplementary Fig. S2). Coinjection of WT BMDMφ with B16.SIY cells significantly accelerated tumor regrowth after 20 Gy compared with 20 Gy alone (1,384 ± 553 mm^3 versus 125 ± 36 mm^3, day 22; P = 0.030; Fig. 2A and B). The regrowth of irradiated tumors in which B16.SIY cells were coinjected with WT BMDMφ occurred significantly earlier compared with irradiated tumors in which B16.SIY cells were

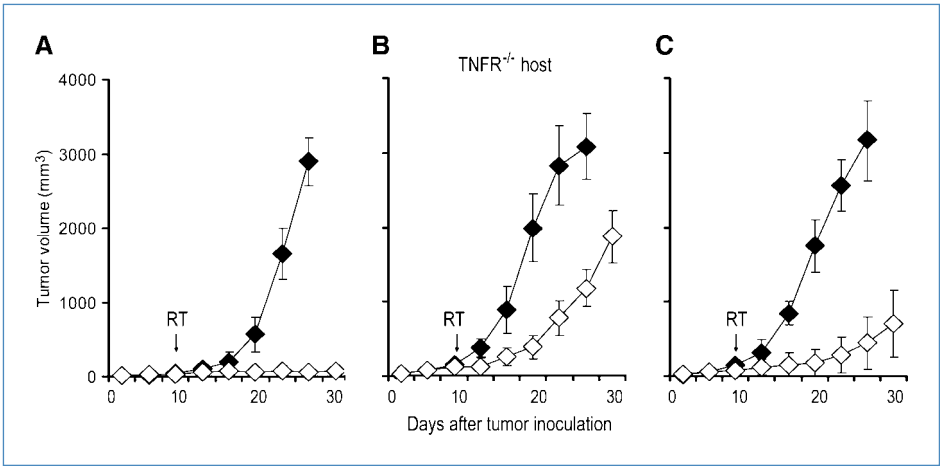

Figure 3. TNFα signaling in BMDMϕ mediates tumor radioresistance through autocrine/paracrine signaling. A, growth of B16.SIY tumors in $TNFR1,2^{-/-}$ mice (n = 15/group). ⧫, B16; ◇, IR in B16. B, coinjection of WT BMDMϕ with B16.SIY cells significantly accelerates tumor regrowth following 20 Gy (P = 0.003, n = 12/group). ⧫, WT macrophage + B16; ◇, IR in WT macrophage + B16. C, coinjection of WT BMDMϕ with B16.SIY cells significantly accelerates tumor regrowth following 20 Gy compared with coinjection of $TNFR1,2^{-/-}$ BMDMϕ and B16.SIY cells (P = 0.041). ⧫, $TNFR^{-/-}$ macrophage + B16; ◇, IR in $TNFR^{-/-}$ macrophage + B16.

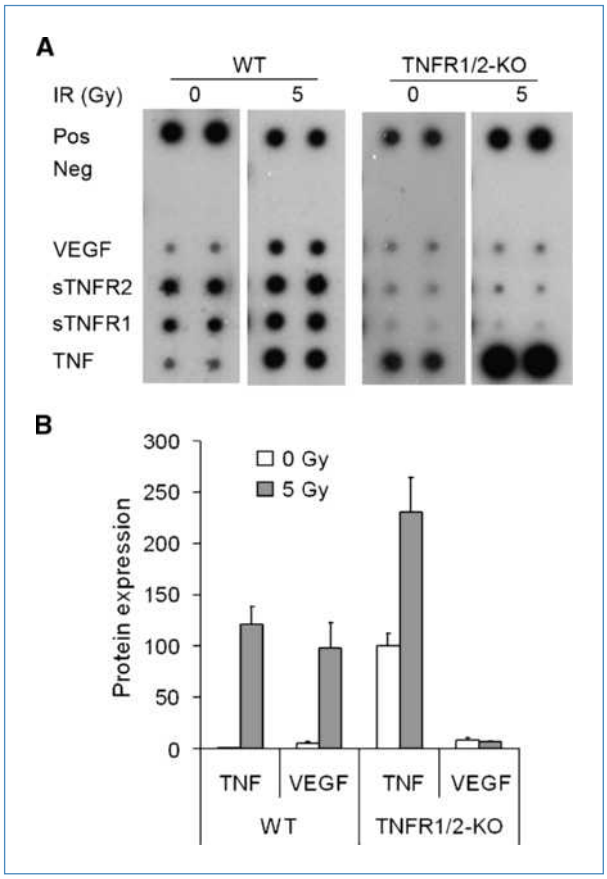

Figure 4. Radiation induction of VEGF in BMDMϕ. A, a significant increase in VEGF was detected in WT BMDMϕ compared with TNFR1, $2^{-/-}$ BMDMϕ with 5 Gy. B, Luminex assay confirmation of VEGF induction by IR in WT BMDMϕ. The mean of triplicates from one representative experiment is shown.

coinjected with $TNF^{-/--/-}$ BMDMφ (1,384 ± 553 mm^3 versus 337 ± 261 mm^3, day 22; $P = 0.037$; Fig. 2B and C). Our data show that depletion of macrophages enhances the antitumor effects of IR and coimplantation of macrophages reverses this effect. These results also implicate macrophage-secreted TNFα in the resistance of tumors to IR and suggest that macrophage-derived TNFα and/or TNFα signaling in TAMφ contributes in part to B16.SIY tumor radioresistance.

TNFα signaling in BMDMφ promotes tumor growth. To investigate the role of TNFα produced specifically by BMDMφ, we injected B16.SIY cells into $TNF^{-/-}$ mice transplanted with WT BM or $TNF^{-/-}$ BM. FACS analysis showed that the BM was reconstituted with >70% of donor cells (Supplementary Fig. S3). Animals underwent macrophage depletion with liposomal clodronate and tumor growth was compared with controls. Tumor volume in WT BM transplant (BMT) mice was significantly reduced by macrophage depletion (3,067 ± 615 mm^3 versus 825 ± 174 mm^3, day 60; $P = 0.017$; Supplementary Fig. S4A). No tumor growth was observed in $TNF^{-/-}$ BMT mice, showing an essential role for TNFα produced by BMDMφ. We next injected B16.SIY cells into TNFR1,$2^{-/-}$ mice after WT or TNFR1,$2^{-/-}$ BMT with or without macrophage depletion. WT BMT in TNFR1,$2^{-/-}$ mice promoted tumor growth 30 days earlier than in TNFR1,$2^{-/-}$ BMT mice, which was significantly delayed when macrophages were depleted (867 ± 64 mm^3 versus 4,353 ± 888 mm^3, day 45; $P = 0.013$; Supplementary Fig. S4B). No significant difference was observed in TNFR1,$2^{-/-}$ mice with TNFR1,$2^{-/-}$ BMT when macrophages were depleted (65 ± 15 mm^3 versus 73 ± 18 mm^3, day 45; $P = 0.549$). In summary, tumors grew more slowly in TNFR1,$2^{-/-}$ BMT mice, whereas WT BMT permitted tumor growth. However, tumor growth was suppressed when macrophages were depleted. These results suggest that autocrine/paracrine TNFα signaling in BMDMφ is essential in promoting tumor growth.

Autocrine/paracrine TNFα signaling in BMDMφ mediates radioresistance. We coinjected BMDMφ from

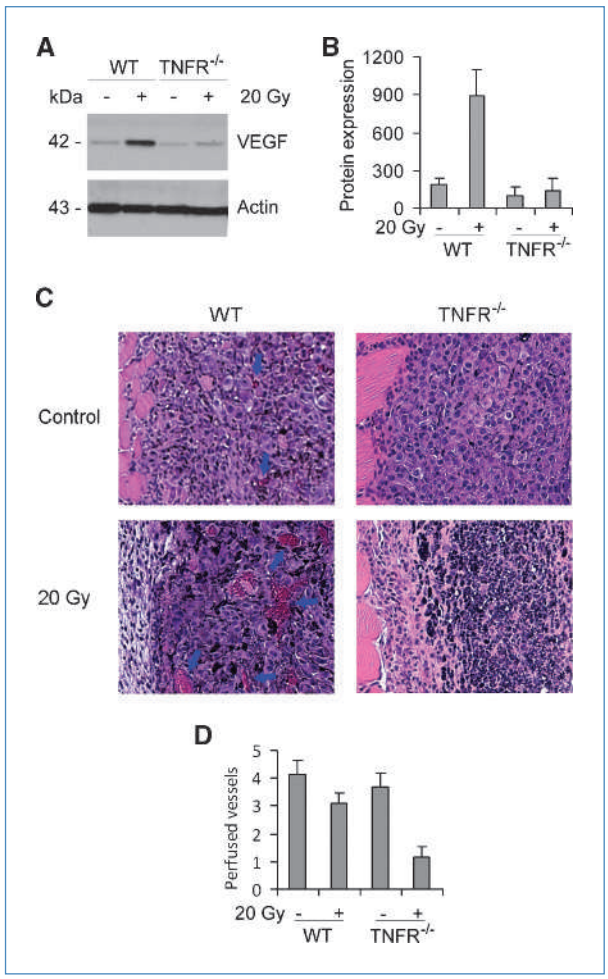

Figure 5. Radiation induction of VEGF in TAMϕ. A, Western blot analysis of VEGF expression of $CD11b^+F4/80^+$ TAMϕ isolated from tumors grown in WT and TNFR1,$2^{-/-}$. B, VEGF levels were significantly elevated in $CD11b^+F4/80^+$ TAMϕ from WT compared with TNFR1,$2^{-/-}$ ($P = 0.015$, Luminex). C, increase neovasculature/angiogenesis in tumors grown in WT compared with TNFR1,$2^{-/-}$ after IR. Arrows indicate functional vessels containing RBCs. D, $VEGFR2^+$ staining shows a significant decrease in perfused vessels after IR in tumors grown in TNFR1,$2^{-/-}$ compared with WT control ($P = 0.0001$) and WT treated with 20 Gy ($P = 0.002$).

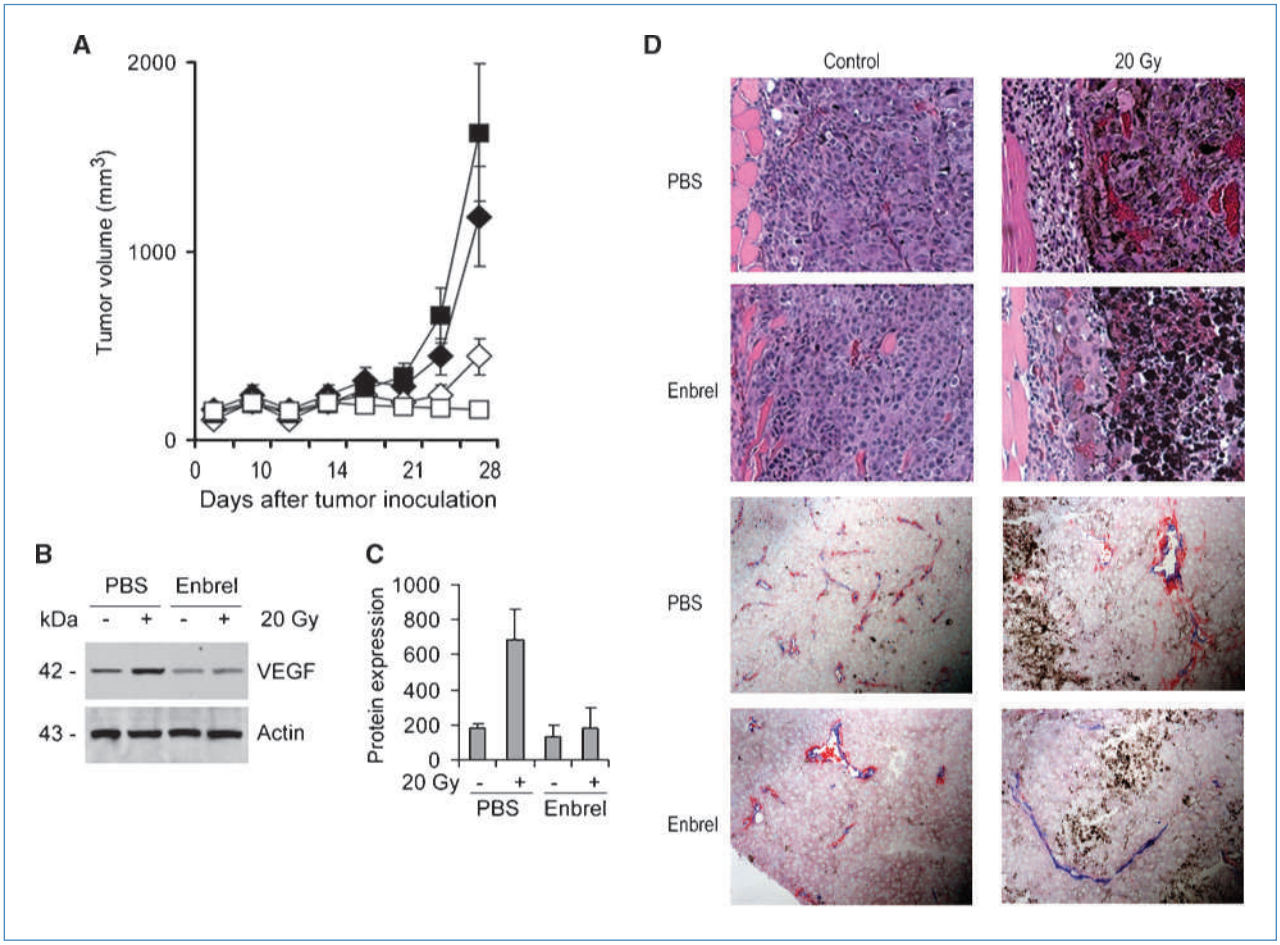

Figure 6. Enbrel enhances radiosensitivity by blocking the VEGF induction in TAMϕ. A, Enbrel + 20 Gy produced a significant decrease in B16.SIY regrowth compared with 20 Gy alone ($P = 0.022$). ♦, PBS; ◇, 20 Gy + PBS; ■, Enbrel; □, 20 Gy + Enbrel. B, Western blot of VEGF expression by $CD11b^+F4/80^+$ TAMϕ from WT treated with Enbrel + 20 Gy. C, Luminex showing inhibition of VEGF induction in $CD11b^+F4/80^+$ TAMϕ isolated from tumors treated with Enbrel + 20 Gy in WT. The mean of triplicates from one representative experiment is shown. D, top, representative tumor tissue sections showing a high density of intact neovasculature/angiogenesis in WT mice after IR and was reduced with IR + Enbrel; bottom, blue $VEGFR2^+$ microvessel density and red $NG2^+$ pericyte coverage were compared between groups. Enbrel + 20 Gy inhibited $VEGFR2^+$ microvessel repair/neovasculature with less pericyte coverage noted by $NG2^+$ staining.

WT or $TNFR1,2^{-/-}$ with B16.SIY cells into $TNFR1,2^{-/-}$ mice. Coinjection of WT BMDMφ significantly accelerated tumor regrowth after 20 Gy compared with IR alone (782 ± 179 mm^3 versus 78 ± 14 mm^3, day 22; $P = 0.003$; Fig. 3A and B). The regrowth of irradiated tumors coinjected with WT BMDMφ was significantly accelerated compared with the response of tumors coinjected with $TNFR1,2^{-/-}$ BMDMφ (782 ± 179 mm^3 versus 283 ± 157 mm^3, day 22; $P = 0.041$; Fig. 3B and C). These results indicate that intact TNF/TNFR signaling in macrophages is required for accelerated tumor regrowth after IR. We repeated these experiments using fractionated IR and report that the growth of tumors coinjected with WT BMDMφ was significantly increased compared with tumors coinjected with $TNFR1,2^{-/-}$ BMDMφ (384 ± 64 mm^3 versus 38 ± 7 mm^3, day 22; $P = 0.010$; Supplementary Fig. S5). These data further suggest that TNFα/TNFR signaling in BMDMφ mediates radioresistance.

BMDMφ supernatant does not affect tumor cell growth or radiosensitivity. We explored the direct effects of BMDMφ on B16.SIY tumor cell radiosensitivity and/or growth *in vitro*. Supernatant from WT BMDMφ suppressed B16.SIY colony formation ($P = 0.015$), whereas supernatant from $TNF^{-/-}$ or $TNFR1,2^{-/-}$ BMDMφ had no effect ($P = 0.259$ and 0.338; Supplementary Fig. S6). Unexpectedly, supernatants from $TNF^{-/-}$ and $TNFR1,2^{-/-}$ BMDMφ cultures increased colony formation in irradiated cells ($P = 0.065$ and 0.055). Interestingly, the radioprotective effect of $TNF^{-/-}$ or $TNFR1,2^{-/-}$ supernatants *in vitro* differs from the *in vivo* findings with $TNF^{-/-}$ or $TNFR1,2^{-/-}$ macrophages. Supernatant from WT BMDMφ had no effect on irradiated B16.SIY colony formation ($P = 0.890$). Supernatant collected from irradiated WT, $TNF^{-/-}$, or $TNFR1,2^{-/-}$ BMDMφ had no significant effect on either control or irradiated B16.SIY growth. These results suggest that the radioprotective effects of TNFα signaling in

BMDMφ are not exerted directly on tumor cells but likely on nontumor cell constituents of the tumor microenvironment.

Induction of VEGF through TNFα/TNFR signaling in TAMφ mediates rapid tumor regrowth following irradiation. In addition to TAMφ, tumor stroma is also composed of matrix proteins and various cell types, including blood/lymphatic vessels (41). Recent data suggest that TAMφ support tumor growth by contributing to angiogenesis and/or vasculogenesis (41–44), in part mediated by TNFα. We used a protein array and examined 62 cytokines and chemokines in unirradiated BMDMφ and BMDMφ treated with 5 Gy. Unirradiated WT and TNFR1,2$^{-/-}$ BMDMφ produced similar cytokine/chemokine levels, including M-CSF, granulocyte CSF, granulocyte macrophage CSF, CCL2, CCL9, IL-6, CXCL2, IL-10, TNFα, and IL-12, and low levels of VEGF. Following 5 Gy, there was a significant increase of VEGF in WT BMDMφ but not TNFR1,2$^{-/-}$ BMDMφ, whereas TNFα was induced in both WT and TNFR1,2$^{-/-}$ BMDMφ (Fig. 4A). These results were confirmed by Luminex (Fig. 4B) and suggest that the induction of VEGF by IR is dependent on TNFα/TNFR autocrine/paracrine signaling in BMDMφ. Our findings support the hypothesis that VEGF production in TAMφ through TNFα signaling activated by IR might play an important role in tumor vessel repair and tumor regrowth.

We examined if irradiation leads to TNF/TNFR-mediated upregulation of VEGF in tumor macrophages. We injected B16.SIY cells into WT and TNFR1,2$^{-/-}$ mice and 20 Gy was delivered when tumors reached 150 to 200 mm^3. Tumors were excised and digested into single-cell suspensions. CD11b$^+$ TAMφ were sorted and VEGF expression was assayed by Western blot and Luminex. Significantly higher levels of VEGF were detected in CD11b$^+$ TAMφ isolated from tumors grown in WT mice compared with TNFR1,2$^{-/-}$ mice ($P = 0.015$; Fig. 5A and B). Increased TAMφ VEGF from tumors in WT mice was mirrored by increased tumor neovasculature/angiogenesis after IR was visualized in H&E- and VEGFR2-stained tissue sections (Fig. 5C). We quantified functional vascular structures showing intact blood perfusion by the presence of RBCs in VEFGR2$^+$ vessels. In tumors grown in TNFR1,2$^{-/-}$ mice, there were significantly decreased functional vessels after IR compared with either untreated control or tumors grown in WT after IR ($P < 0.0001$ and $P = 0.002$, respectively; Fig. 5D). In addition, more surviving tumor cells exhibiting intact morphology were present in irradiated tumors in WT compared with tumors in TNFR1,2$^{-/-}$, which showed greater radiosensitivity.

Depleting TNFα with Enbrel enhances tumor radiosensitivity. To test this hypothesis that TNFα blockade might be clinically relevant, we injected B16.SIY cells into WT mice and treated them with Enbrel + 20 Gy (32, 33). Enbrel-treated animals had slightly larger tumors than untreated control animals. Mice treated with Enbrel + 20 Gy exhibited a reduction in tumor regrowth compared with 20 Gy alone (153 ± 34 mm^3 versus 440 ± 97 mm^3, day 28; $P = 0.022$; Fig. 6A).

The observation that IR induced VEGF production by macrophages via TNFα/TNFR signaling pathways led us to examine the effect of pharmacologic TNFα inhibition and radiation on tumor angiogenesis. As with genetic deletion of TNFR1,2, Enbrel treatment prevented upregulation of VEGF by tumor macrophages *in vivo* (Fig. 6B and C). We next assessed the effect of IR + Enbrel on neovascularization. Radiation alone led to a significant reduction in microvessel density as measured by VEGFR2$^+$ [PBS (24 ± 1.8) versus PBS + IR (4.1 ± 1.4); $P < 0.0001$]. Enbrel alone led to a modest decrease in microvessel density [PBS (24 ± 1.8) versus Enbrel (13 ± 1); $P < 0.01$], whereas Enbrel + IR significantly inhibited angiogenesis when compared with all groups (2.75 ± 0.35 versus Enbrel alone, 13 ± 1, $P < 0.0001$; versus PBS + IR, 4.1 ± 1.4, $P < 0.01$; Fig. 6D). NG2$^+$ pericyte coverage was reduced in tumors treated with Enbrel compared with PBS (84 ± 2.3% versus 98 ± 0.2%; $P < 0.001$) and further decreased with Enbrel + IR (57 ± 22.4%; $P = 0.03$, compared with Enbrel alone). Vascular size and morphology were also substantially affected by treatment. For example, Enbrel + IR–treated tumors showed narrow lumens suggestive of vascular collapse. Finally, whereas radiation exposure led to vascular hemorrhage, the addition of Enbrel intensified hemorrhagic necrosis and regression. These data show a profound effect of TNFα depletion + IR on angiogenesis and vascular function. Given that irradiated macrophages upregulated VEGF expression, we next hypothesized that blockade of VEGF would likewise enhance radiosensitivity. Treatment of mice with neutralizing antibodies to VEGF led to increased radiosensitivity in B16F1 (806.1 ± 329.1 versus IR alone, 2,101.8 ± 525.4; $P = 0.05$) and B16.SIY (0.5 ± 0.1 versus IR alone, 408.5 ± 65.1; $P = 0.005$) tumors (Supplementary Fig. S7; ref. 38).

Discussion

We tested the hypothesis that depletion of TAMφ by liposomal clodronate would improve the antitumor effects of radiotherapy as determined by a delay of tumor regrowth. The effects of macrophage depletion were most marked when macrophages were depleted before tumors were established. TAMφ have been reported to secrete a variety of cytokines and other proteins that promote tumor growth. Our results show that the intact TNFα/TNFR signaling in TAMφ is important in the autocrine/paracrine secretion of cytokines by BMDMφ. TNFα is a proinflammatory cytokine that is cytotoxic to some tumor cell lines and tumors *in vivo* in high concentrations (45, 46). In our study, we were unable to show that radioresistance was mediated by a direct effect on B16.SIY cells using supernatant from WT BMDMφ. This raised the possibility that TNFα-stimulated TAMφ promoted radioresistance by effects on the tumor microenvironment. TNFα at physiologic concentrations has recently been implicated in cancer induction and support of tumor angiogenesis, in part, through the attraction of BM-derived myeloid precursor cells that contribute to tumor blood vessel formation and stabilization (42, 47). We investigated if TNF/TNFR signaling in macrophages regulates the production of angiogenic cytokines by irradiated macrophages. Our data show that inhibition of TNFR signaling by both genetic and pharmacologic means prevents increased production of VEGF by irradiated macrophages. Immunohistochemical analyses show that the combination of TNFα inhibition plus IR led

to both significant decreases in neovascularization as well as vascular function as evidenced by reduced pericyte coverage and increased hemorrhage.

A recent report noted that macrophage-secreted VEGF paradoxically slowed tumor growth in part by inducing tumor vessel abnormalities, such as tortuosity and leakiness, resulting in tumor hypoxia, whereas tumor-secreted VEGF "normalized" tumor vasculature (48). Interestingly, when macrophage VEGF was deleted, tumors grew more rapidly due to a more "normalized" vasculature but were also more sensitive to cyclophosphamide. Our results are consistent with this report, showing the Enbrel-treated tumors were actually more sensitive to IR. In contrast to the report of Stockmann and colleagues (48), TNFα blockade did not increase vessel pericyte coverage, suggesting that TNFR signaling in tumor macrophages likely affects several angiogenic pathways in addition to VEGF. Nonetheless, blockade of VEGF upregulation by inhibition of TNFα signaling represents an alternative clinically relevant method to enhance radiosensitivity via targeting of TAMφ. Paradoxically, supernatant from macrophages defective in TNF signaling through germline deletions in TNF or TNFR1,2 conferred modest radioprotection on B16.SIY cells *in vitro* through an unknown mechanism. Together, these data suggest that macrophage blockade mediates *in vivo* radiosensitivity predominantly through effects on the microenvironment. Active TNFα signaling in irradiated macrophages seems necessary for upregulation of macrophage-derived VEGF, resulting in enhanced preservation of the irradiated vasculature.

Tumor angiogenesis is distinguished from postnatal vasculogenesis in that tumor angiogenesis is proposed to occur through endothelial migration and sprouting from preexisting blood vessels, whereas vasculogenesis is proposed to occur by the recruitment of BM cells to the site of tumor angiogenesis or local inflammatory damage. Although vasculogenesis was previously described as direct incorporation of progenitor cells into newly emerging vasculature, it also involves the recruitment of BM-derived angiogenic populations that enhance angiogenesis through paracrine mechanisms. The extent to which tumor neovascularization depends on local endothelial cells or infiltrating angiogenic cells is controversial. Recently, tumor regrowth by local myelomonocytic $CD11b^+$ cells was reported to induce tumor vasculogenesis following irradiation through secretion of matrix metalloproteinase-9 in a model where tumor angiogenesis was suppressed by prior irradiation of the tumor bed (25). Additionally TAMφ secrete a variety of proangiogenic proteins, including IL-8, TNFα, and VEGF. Therefore, both angiogenesis and vasculogenesis may be supported by TAMφ-derived factors. Whereas our data using Enbrel suggest that pharmacologic inhibition of macrophage TNFR signaling enhances radiosensitivity, our liposomal clodronate data show that reducing macrophage populations in tumors represents another potential antiangiogenic and antivasculogenic strategy. Systemically delivering liposomal clodronate to patients may not be feasible. However, CSF-1 receptor kinase inhibitors may block macrophage differentiation and function, providing an alternative biological tool to inhibit proinflammatory cytokine production from macrophages (49). The availability of these small molecules and monoclonal antibodies targeting either CSF-1R or CSF-1 to deplete TAMφ number and function may allow us to translate these strategies to promote radiosensitivity in future studies.

We also report that blocking VEGF enhances the effect of IR (38, 50). Although anti-VEGF therapy could block VEGF derived from either vasculogenic myeloid populations or tumor cells, our results confirm that direct VEGF blockade is another therapeutic strategy to increase radiosensitivity. Despite the clear correlation between tumor vascularization and VEGF expression, TNF can also modulate the expression of other antiangiogenic factors, including thrombospondin and angiostatic chemokines such as CXCL10 and CXCL9. Therefore, targeting the TNFα/TNFR signaling in TAMφ may enhance radiosensitivity through additional pathways beyond VEGF signaling.

In summary, we used both genetic and pharmacologic inhibition of TNFα signaling to study the role of tumor macrophages in promoting tumor radioresistance. Rather than directly affecting tumor cells, active TNFα signaling in irradiated macrophages results in the production of angiogenic cytokines such as VEGF. We have used coimplantation models to show that macrophages are sufficient for this effect and liposomal clodronate to show that macrophages are required. Although liposomal clodronate might have off-target cellular affects, previous studies suggest that liposomal clodronate selectively depletes macrophages as opposed to other hematopoietic cells. Because the effects of liposomal clodronate on other stromal components remain unclear, we also used BM transplantation studies together with liposomal clodronate to study the effects of depletion of BM-derived cells. It nonetheless remains possible that active TNFα signaling in cellular components of the microenvironment might mediate radioresistance as well. Other limitations of our study include (*a*) the lack of a tissue-specific promoter such as LysM to delete TNFα specifically in myeloid cells, (*b*) identification of which BMDMφ populations (M1 versus M2) mediate tumor vascular formation/stabilization following IR, and (*c*) whether VEGF secreted by macrophages attracts additional local angiogenic cells, which contribute to tumor vascularization and regrowth following radiotherapy. In spite of these caveats, our results suggest that blockade of TNF/TNFR signaling in TAMφ is an attractive target to improve the efficacy of radiotherapy.

Disclosure of Potential Conflicts of Interest

No potential conflicts of interest were disclosed.

Grant Support

National Cancer Institute grant CA111423 (R.R. Weichselbaum) and National Heart, Lung and Blood Institute grant K08HL071938 (K.S. Cohen).

The costs of publication of this article were defrayed in part by the payment of page charges. This article must therefore be hereby marked *advertisement* in accordance with 18 U.S.C. Section 1734 solely to indicate this fact.

Received 8/11/09; revised 11/16/09; accepted 12/9/09; published OnlineFirst 2/9/10.

References

1. Salama JK CS, Mehta N, Yenice KM, et al. An initial report of a radiation dose escalation trial in patients with one to five sites of metastatic disease. Clin Cancer Res 2008;14:5255–9.
2. Vokes EE, Panje WR, Mick R, et al. A randomized study comparing two regimens of neoadjuvant and adjuvant chemotherapy in multimodal therapy for locally advanced head and neck cancer. Cancer 1990;66:206–13.
3. Masunaga S, Hirayama R, Uzawa A, et al. The effect of post-irradiation tumor oxygenation status on recovery from radiation-induced damage *in vivo*: with reference to that in quiescent cell populations. J Cancer Res Clin Oncol 2009;135:1109–16.
4. Hwang RF, Moore T, Arumugam T, et al. Cancer-associated stromal fibroblasts promote pancreatic tumor progression. Cancer Res 2008; 68:918–26.
5. Roses RE, Xu M, Koski GK, Czerniecki BJ. Radiation therapy and Toll-like receptor signaling: implications for the treatment of cancer. Oncogene 2008;27:200–7.
6. Jain RK. Lessons from multidisciplinary translational trials on anti-angiogenic therapy of cancer. Nat Rev Cancer 2008;8:309–16.
7. Senan S, Smit EF. Design of clinical trials of radiation combined with antiangiogenic therapy. Oncologist 2007;12:465–77.
8. Crane CH, Ellis LM, Abbruzzese JL, et al. Phase I trial evaluating the safety of bevacizumab with concurrent radiotherapy and capecitabine in locally advanced pancreatic cancer. J Clin Oncol 2006;24: 1145–51.
9. Duda DG, Jain RK, Willett CG. Antiangiogenics: the potential role of integrating this novel treatment modality with chemoradiation for solid cancers. J Clin Oncol 2007;25:4033–42.
10. Gutin PH, Iwamoto FM, Beal K, et al. Safety and efficacy of bevacizumab with hypofractionated stereotactic irradiation for recurrent malignant gliomas. Int J Radiat Oncol Biol Phys 2009;75:156–63.
11. Seiwert TY, Haraf DJ, Cohen EE, et al. Phase I study of bevacizumab added to fluorouracil- and hydroxyurea-based concomitant chemoradiotherapy for poor-prognosis head and neck cancer. J Clin Oncol 2008;26:1732–41.
12. Paez-Ribes M, Allen E, Hudock J, et al. Antiangiogenic therapy elicits malignant progression of tumors to increased local invasion and distant metastasis. Cancer Cell 2009;15:220–31.
13. Ebos JM, Lee CR, Cruz-Munoz W, et al. Accelerated metastasis after short-term treatment with a potent inhibitor of tumor angiogenesis. Cancer Cell 2009;15:232–9.
14. Allavena P, Sica A, Solinas G, Porta C, Mantovani A. The inflammatory micro-environment in tumor progression: the role of tumor-associated macrophages. Crit Rev Oncol Hematol 2008;66:1–9.
15. Murdoch C, Muthana M, Coffelt SB, Lewis CE. The role of myeloid cells in the promotion of tumour angiogenesis. Nat Rev Cancer 2008; 8:618–31.
16. Serafini P, Borrello I, Bronte V. Myeloid suppressor cells in cancer: recruitment, phenotype, properties, and mechanisms of immune suppression. Semin Cancer Biol 2006;16:53–65.
17. Lambert LE, Paulnock DM. Modulation of macrophage function by γ-irradiation. Acquisition of the primed cell intermediate stage of the macrophage tumoricidal activation pathway. J Immunol 1987; 139:2834–41.
18. Fulton AM, Chong YC. The role of macrophage-derived TNFα in the induction of sublethal tumor cell DNA damage. Carcinogenesis 1992; 13:77–81.
19. Ibuki Y, Goto R. Augmentation of NO production and cytolytic activity of Mϕ obtained from mice irradiated with a low dose of γ-rays. J Radiat Res 1995;36:209–20.
20. Weichselbaum RR, Kufe DW, Hellman S, et al. Radiation-induced tumour necrosis factor-α expression: clinical application of transcriptional and physical targeting of gene therapy. Lancet Oncol 2002;3: 665–71.
21. Milas L, Wike J, Hunter N, Volpe J, Basic I. Macrophage content of murine sarcomas and carcinomas: associations with tumor growth parameters and tumor radiocurability. Cancer Res 1987; 47:1069–75.
22. Milas L. Tumor bed effect in murine tumors: relationship to tumor take and tumor macrophage content. Radiat Res 1990; 123:232–6.
23. Du R, Lu KV, Petritsch C, et al. HIF1α induces the recruitment of bone marrow-derived vascular modulatory cells to regulate tumor angiogenesis and invasion. Cancer Cell 2008;13:206–20.
24. Tsai CS, Chen FH, Wang CC, et al. Macrophages from irradiated tumors express higher levels of iNOS, arginase-I and COX-2, and promote tumor growth. Int J Radiat Oncol Biol Phys 2007;68: 499–507.
25. Ahn GO, Brown JM. Matrix metalloproteinase-9 is required for tumor vasculogenesis but not for angiogenesis: role of bone marrow-derived myelomonocytic cells. Cancer Cell 2008;13:193–205.
26. Kim S, Takahashi H, Lin WW, et al. Carcinoma-produced factors activate myeloid cells through TLR2 to stimulate metastasis. Nature 2009;457:102–6.
27. Li B, Vincent A, Cates J, Brantley-Sieders DM, Polk DB, Young PP. Low levels of tumor necrosis factor α increase tumor growth by inducing an endothelial phenotype of monocytes recruited to the tumor site. Cancer Res 2009;69:338–48.
28. Mantovani A, Allavena P, Sica A, Balkwill F. Cancer-related inflammation. Nature 2008;454:436–44.
29. Balkwill F. Tumour necrosis factor and cancer. Nat Rev Cancer 2009; 9:361–71.
30. Sherman ML, Datta R, Hallahan DE, Weichselbaum RR, Kufe DW. Regulation of tumor necrosis factor gene expression by ionizing radiation in human myeloid leukemia cells and peripheral blood monocytes. J Clin Invest 1991;87:1794–7.
31. Weichselbaum RR, Hallahan DE, Sukhatme VP, Kufe DW. Gene therapy targeted by ionizing radiation. Int J Radiat Oncol Biol Phys 1992; 24:565–7.
32. Grounds MD, Davies M, Torrisi J, Shavlakadze T, White J, Hodgetts S. Silencing TNFα activity by using Remicade or Enbrel blocks inflammation in whole muscle grafts: an *in vivo* bioassay to assess the efficacy of anti-cytokine drugs in mice. Cell Tissue Res 2005; 320:509–15.
33. Wolthuis EK, Vlaar AP, Choi G, et al. Recombinant human soluble tumor necrosis factor-α receptor fusion protein partly attenuates ventilator-induced lung injury. Shock 2009;31:262–6.
34. Scott KA, Moore RJ, Arnott CH, et al. An anti-tumor necrosis factor-α antibody inhibits the development of experimental skin tumors. Mol Cancer Ther 2003;2:445–51.
35. Mauceri HJ, Beckett MA, Liang H, et al. Translational strategies exploiting TNF-α that sensitize tumors to radiation therapy. Cancer Gene Ther 2009;16:373–81.
36. Gazzaniga S, Bravo AI, Guglielmotti A, et al. Targeting tumor-associated macrophages and inhibition of MCP-1 reduce angiogenesis and tumor growth in a human melanoma xenograft. J Invest Dermatol 2007;127:2031–41.
37. Van Rooijen N, Sanders A. Liposome mediated depletion of macrophages: mechanism of action, preparation of liposomes and applications. J Immunol Methods 1994;174:83–93.
38. Gorski DH, Beckett MA, Jaskowiak NT, et al. Blockage of the vascular endothelial growth factor stress response increases the antitumor effects of ionizing radiation. Cancer Res 1999;59: 3374–8.
39. van Rooijen N, Sanders A, van den Berg TK. Apoptosis of macrophages induced by liposome-mediated intracellular delivery of clodronate and propamidine. J Immunol Methods 1996;193: 93–9.
40. Miselis NR, Wu ZJ, Van Rooijen N, Kane AB. Targeting tumor-associated macrophages in an orthotopic murine model of diffuse malignant mesothelioma. Mol Cancer Ther 2008;7:788–99.
41. Coussens LM, Werb Z. Inflammation and cancer. Nature 2002;420: 860–7.
42. Balkwill F, Charles KA, Mantovani A. Smoldering and polarized inflammation in the initiation and promotion of malignant disease. Cancer Cell 2005;7:211–7.
43. Pollard JW. Tumour-educated macrophages promote tumour progression and metastasis. Nat Rev Cancer 2004;4:71–8.

44. de Visser KE, Eichten A, Coussens LM. Paradoxical roles of the immune system during cancer development. Nat Rev Cancer 2006; 6:24–37.

45. Menon C, Bauer TW, Kelley ST, et al. Tumoricidal activity of high-dose tumor necrosis factor-α is mediated by macrophage-derived nitric oxide burst and permanent blood flow shutdown. Int J Cancer 2008;123:464–75.

46. Havell EA, Fiers W, North RJ. The antitumor function of tumor necrosis factor (TNF). I. Therapeutic action of TNF against an established murine sarcoma is indirect, immunologically dependent, and limited by severe toxicity. J Exp Med 1988;167: 1067–85.

47. Moore RJ, Owens DM, Stamp G, et al. Mice deficient in tumor necrosis factor-α are resistant to skin carcinogenesis. Nat Med 1999;5:828–31.

48. Stockmann C, Doedens A, Weidemann A, et al. Deletion of vascular endothelial growth factor in myeloid cells accelerates tumorigenesis. Nature 2008;456:814–8.

49. Irvine KM, Burns CJ, Wilks AF, Su S, Hume DA, Sweet MJ. A CSF-1 receptor kinase inhibitor targets effector functions and inhibits pro-inflammatory cytokine production from murine macrophage populations. FASEB J 2006;20:1921–3.

50. Zwolak P, Dudek AZ, Bodempudi VD, et al. Local irradiation in combination with bevacizumab enhances radiation control of bone destruction and cancer-induced pain in a model of bone metastases. Int J Cancer 2008;122:681–8.